ACS Catalysis

Research Article

pubs.acs.org/acscatalysis

Intermetallic Alloys as CO Electroreduction Catalysts—Role of Isolated Active Sites

Mohammadreza Karamad, Vladimir Tripkovic,* and Jan Rossmeisl

Center for Atomic-scale Materials Design, Department of Physics, Technical University of Denmark, Fysikvej, Building 311, DK-2800 Kongens Lyngby, Denmark

Supporting Information

ABSTRACT: One of the main challenges associated with the electrochemical CO or CO_2 reduction is poor selectivity toward energetically rich products. In order to promote selectivity toward hydrocarbons and alcohols, most notably, the hydrogen evolution reaction (HER) should be suppressed. To achieve this goal, we studied intermetallic compounds consisting of transition metal (TM) elements that can reduce CO (Ru, Co, Rh, Ir, Ni, Pd, Pt, and Cu) separated by TM and post transition metal elements (Ag, Au, Cd, Zn, Hg, In, Sn, Pb, Sb, and Bi) that are very poor HER catalysts. In total, 34 different stable binary bulk alloys forming from these elements have been investigated using density functional theory calculations. The electronic and geometric properties of the catalyst surface can be tuned by varying the size of the active centers and the elements forming them. We have identified six different potentially selective intermetallic surfaces on which CO can be reduced to methanol at potentials comparable to or even slightly positive than those for CO/CO_2 reduction to methane on Cu. Common features shared by most of the selective alloys are single TM sites. The role of single sites is to block parasitic HER and thereby promote CO reduction.

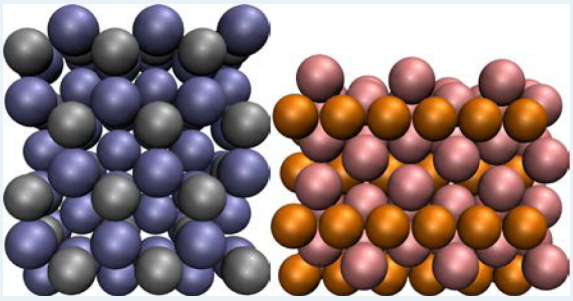

KEYWORDS: *alloys, intermetallics, CO_2 reduction, CO reduction, density functional theory, single sites*

INTRODUCTION

The electrochemical reduction (ER) of CO_2/CO to hydrocarbons and alcohols using intermittent renewable energy sources is a promising approach to store energy into chemical bonds for automotive and industrial applications.[1] The conversion of CO_2 to fuels would at the same time benefit the environment by reducing the carbon footprint.[2] In the past, research efforts were concentrated on understanding the mechanism through which the ER of CO/CO_2 proceeds.[3−11] Hori was the first one to report reaction products categorized by the ability of metals to bind CO and hydrogen.[3,4] According to his classification, formate is the primary product on metals with weak hydrogen and CO binding energies (Hg, Cd, or Pb). Metals with weak hydrogen and strong CO binding energies (Pt, Ni, or Fe) reduce CO/CO_2 to tightly adsorbed CO. As high overpotentials are required for further CO reduction, the primary reduction product for this group is hydrogen. The only metals that can catalyze the carbon−oxygen bond breaking in CO/CO_2 are those with moderate binding energies of CO and hydrogen (Cu, Au, and Ag). Cu is the only metal on which CO is reduced to hydrocarbons in significant amounts, albeit accompanied by a very high overpotential.[4,9]

There are three criteria that should be fulfilled in pursuit for new catalyst materials: (1) the stability criterion—the catalyst should be stable at potentials of interest so that the activity does not degrade over time; (2) the selectivity criterion—the catalyst should have a high selectivity toward desired products (i.e. a high Faradaic efficiency); and (3) the activity criterion—the catalyst should have a high energy efficiency (i.e., a low reduction overpotential).[12]

The selectivity and activity toward hydrogen evolution reaction (HER) and ER of CO/CO_2 can be controlled via two effects: electronic effect and geometric effect.[13−18] The change of electronic effect is accomplished by means of alloying, in which chemical properties of a host element are altered by addition of a foreign element. This change can take place either through a ligand effect (vertical electronic effect)[19−23] or stress (horizontal electronic effect).[19,24] Changes in electronic properties would reflect on the binding energies of H* and different intermediates involved in the ER of CO/CO_2. This could give rise to a catalytic activity and selectivity that is different from that of constituent elements.[22] The geometric effect arises when an adsorbate assumes a different binding site due to a change in surface geometry. Another plausible way to change the binding site is to vary the number of atoms in small surface assemblies. This particular geometric effect is also known as the ensemble effect. The ensemble effect can have a profound influence on the activity, which has been well-documented in the past.[13−15,18,25−28] For example, methanol and CO oxidation are very similar reactions in the sense that they both proceed

Received: March 13, 2014
Revised: May 27, 2014
Published: June 2, 2014

   dx.doi.org/10.1021/cs500328c | ACS Catal. 2014, 4, 2268−2273

through a CO intermediate. Pt_3Sn, which is very active for CO oxidation, is at the same time a very poor catalyst for methanol oxidation because of an insufficient number of free Pt atoms required for breaking the C−H bond.[25]

In the present study, we exploit the changes in the electronic and geometric effects with the aim to pinpoint new catalytic materials for the ER of CO/CO_2. The strategy we propose is based on our current theoretical understanding of catalytic activity of different metal elements toward HER and CO/CO_2 reduction.[9,10,29,30] We set out to screen for new alloy catalysts of type A_xB_y, where element A is a metal capable of catalyzing the ER of CO_2 and element B is a metal that is poor for HER and CO/CO_2 reduction. For element A, we chose late transition metals (TMs) (i.e., Ru, Co, Rh, Ir, Ni, Pd, Pt, and Cu) and for element B, TMs (Ag, Au) and post-transition metals (PTM) (Cd, Zn, Hg, In, Sn, Pb, Sb, and Bi).[4] To study the ensemble effect, the alloys were classified into two groups based on the distribution of the TM atoms on the surface: (1) alloys with isolated TM sites, where a single metal A is completely surrounded by atoms B and (2) metal A forms rows of atoms (every atom A has two nearest neighbors of the same type) embedded in the "sea" of metal B. The snapshots of the structures, representatives of the alloys with single active sites and active rows of atoms are shown in Figure 1.

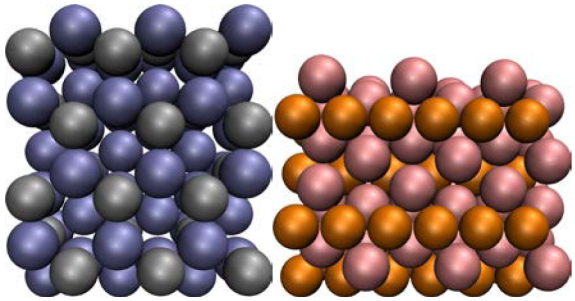

Figure 1. Top views of (left) $PtIn_2(111)$ and (right) $PdPb_2(100)$ intermetallic alloys illustrating the arrangement of active sites in single atom islands and rows, respectively. Dark blue and orange atoms are active Pt and Pd sites, and blue and pink atoms are inert In and Pb sites, respectively.

The alloy surfaces with high A content were excluded because they resemble pure A solid phases, which with exception of copper are not generally considered to be active for the ER of CO/CO_2.[4] The alloy selection principle is best illustrated with an example. According to the phase diagram, Pt and Sn form five stable alloys PtSn, $PtSn_2$, $PtSn_4$, Pt_3Sn, and Pt_3Sn_2, depending on their mutual ratios. First, three alloys are Sn-rich phases, and the last two are Pt-rich phases. The Pt-rich phases are excluded from the screening, because they mimic pure Pt, which produces only hydrogen.[4]

The concept of isolated reaction centers is not new. It has previously been applied for the ER of CO_2 on nonmetallic catalysts and also for oxygen reduction reaction on metal catalysts.[31,32] Recently, we have also examined various metal-functionalized porphyrin-like graphene catalysts for the ER of CO.[31] This study prompted us to study metallic systems that share similar features with these graphene−porphyrin composites.

In this work, we set about to investigate the CO_2/CO ER selectivity and activity by examining binary alloys forming from metals that are capable of catalyzing this reaction and metals that have poor HER activity. Establishing a selectivity criterion and estimating activities led us to the discovery of several alloys potentially active and selective for the ER of CO.

COMPUTATIONAL DETAILS

The total energies of different surfaces with adsorbates were calculated with density functional theory (DFT) calculations employing the grid-based projector-augmented wave method (GPAW) code integrated with Atomic Simulation Environment (ASE).[33] The calculations were performed using the RPBE exchange-correlation functional[34] and the grid spacing of 0.17 Å. The occupation of one-electron states was calculated at an electronic temperature of k_BT = 0.1 eV, and subsequently, all the energies were extrapolated to T = 0 K.

Extended model slabs were constructed for all surfaces considered in this study. Successive slabs in the surface normal direction were separated by at least 12 Å of vacuum. In all the calculations, the adsorption was only allowed on one side of the slab. All adsorption sites were considered, and only the most stable ones are reported here. Zero point energies and entropies were taken from ref 35. For each bulk binary alloy, the lattice constants were optimized within its crystal system. The most stable surface structure for each alloy has been either taken from the literature or determined on the basis of the crystal structure the alloy assumes. More details about the structures and computational parameters are found in Supporting Information.

The computational hydrogen electrode (CHE) method introduced in ref 36 was used to calculate the free energy levels of all intermediate states. According to this model, the chemical potential of protons and electrons is taken into account by shifting the free energy levels of adsorbates by −eU − 2.303kTpH. The potential at which an electrochemical reaction takes place is defined as the maximum absolute free energy difference between any two successive electrochemical steps. The overpotential is obtained when the theoretical potential at which all electrochemical steps become downhill in free energy is subtracted from the reaction's equilibrium potential.

A recent study showed that the RPBE functional is poor in describing the reaction energy of gas-phase molecules containing the OCO backbone.[9] Very recently, we have performed a similar kind of analysis[31] and determined that the mean absolute error for the gas-phase molecules containing the OCO backbone amounts to 0.43 eV. We note that such correction only applies to gas phase molecules (i.e., in our case CO_2) and not to the adsorbed species, such as COOH* or *OCHO.[9]

The effects of solvation and electric field have not been explicitly considered. It is important to note that for polar intermediates (COOH, CH_2OH, or COH), in particular, these effects are non-negligible. The usual estimates for water-induced stabilization are around 0.3 eV, although the exact value depends on the surface morphology, polarity, and orientation of the intermediate. We will argue how the value of ca. 0.3 eV could influence reaction products and overpotentials. Because COH and OH as well as COOH and OOH have very similar adsorption configurations, one can assume the same electric field corrections for COH and COOH as for OH and OOH. These amount to 0.03 and −0.05 eV at −1.0 V, respectively.[37,38] These corrections are neglected hereafter as their energies are rather small and become even smaller when potential is increased positively.

Another problem encountered in DFT calculations is that the CO binding energy on TM surfaces is usually overestimated.[39−41] The reason for this overestimation is because charge donation and back-donation between CO and the metal surface are poorly described within standard DFT. To resolve this issue, an empirical correction has been devised on the basis of the internal stretching mode of CO.[39−41] This correction is usually significant for higher symmetry binding sites (fcc, hcp, and bridge), whereas for the binding in the on-top position, it is less than 0.1 eV. The correction will act to reduce the free potential barrier for the reaction by the equal amount. As CO on most of the alloys (all single site alloys) adsorbs in the on-top configuration, we decided not to include this correction.

It is important to stress that we have just investigated the most stable crystal termination which we inferred either by looking in the literature or by cutting the crystal in such a way that the least number of bonds is

dx.doi.org/10.1021/cs500328c | ACS Catal. 2014, 4, 2268−2273

cleaved. Thus, the obtained surface corresponds to the surface with the lowest free energy. The list of binary alloys and studied crystal terminations is compiled in Supporting Information.

Finally, the simple thermochemical analysis based on the CHE method has previously proven valuable in predicting new electrocatalysts for different reactions.[17,22,24,30,42] However, the inclusion of all the details of the solid/aqueous interface (electric field, water environment, etc.) is necessary to obtain correct reaction rates.

RESULTS AND DISCUSSION

The ER of CO_2 results in a range of different products. The product distribution strongly depends on the electrode material and potential.[2,4] The main reactions are shown below along with their equilibrium potentials versus the reversible hydrogen electrode (RHE).[43]

$$H^+ + e^- \rightarrow 1/2H_2(g) \quad U = 0.0V \tag{1}$$

$$CO_2 + 2(H^+ + e^-) \rightarrow HCOOH(aq) \quad U = -0.20V \tag{2}$$

$$CO_2 + 2(H^+ + e^-) \rightarrow CO(g) + H_2O \quad U = -0.12V \tag{3}$$

$$CO_2 + 4(H^+ + e^-) \rightarrow CH_2O(aq) + H_2O \quad U = -0.07V \tag{4}$$

$$CO_2 + 6(H^+ + e^-) \rightarrow CH_3OH(aq) + H_2O \quad U = 0.03V \tag{5}$$

$$CO_2 + 8(H^+ + e^-) \rightarrow CH_4(g) + 2H_2O \quad U = 0.17V \tag{6}$$

From a thermodynamic standpoint, the HER (reaction 1) occurs at U = 0 V versus RHE. Although the equilibrium potentials for the ER of CO_2 to methanol or methane (reactions 5 and 6) are higher than 0 V, for example, at negative potentials, HER will most likely prevail due to a much lower reaction overpotential.[29,44]

Stability. The choice of the catalysts was guided by two rules. First, the alloys should not form oxides or dissolve at potentials below 0 V versus RHE,[45] and second, the alloys should be intrinsically stable. The first condition was imposed by selecting the elements that have positive or slightly negative dissolution potentials. In any case, these dissolution potentials are higher than the potentials at which CO_2/CO reduction commences. With respect to the second condition, we have calculated formation energies of intermetallic compounds and plotted them against the CO binding energies. The results are presented in Figure 2. As can be seen, except for a few alloys, most of the intermetallic alloys have either negative or at least zero energies of formation.

We would like to emphasize that in order to retain high catalytic activity and selectivity over time, the surface composition should not change during the electrochemical reaction. The surface composition could be different from the bulk composition, owing to segregation effects, that is, the migration of one alloy component from the bulk to the surface. It is well-established that strong interaction of adsorbates with one of the alloy components could trigger segregation.[28,46−48] This, in turn, could affect the catalytic activity and selectivity. Most of these alloys belong to the class of alloys called intermetallics. What distinguishes intermetallics from ordinary alloys is that they have rather fixed stoichiometries, meaning that the atom diffusion is limited. "Regular" alloys form solid solutions of two

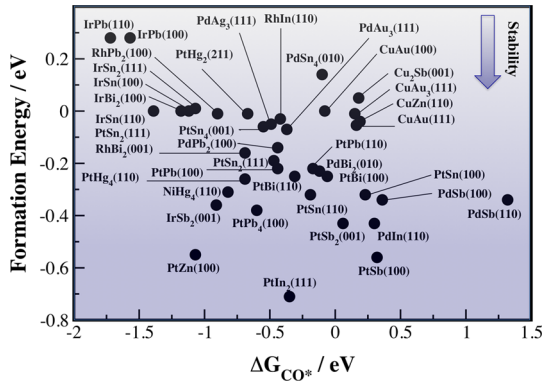

Figure 2. Normalized formation energies of intermetallic alloys with respect to the number of atoms in the bulk unit cell plotted as a function of the CO binding energy. The color gradient scale shows how stability is changing; darker tones mean higher stability.

or more metals with surface and bulk compositions that are varying with time. A simple rule of thumb is that the alloys between transition metals that commonly assume face-centered cubic crystal structure form regular alloys, whereas the alloys between transition and s or p metals form intermetallic compounds which might belong to any crystal system. Because intermetallic alloys have rather fixed compositions, it is reasonable to assume that their activities and selectivities will be less subject to changes than in the regular alloys.

Selectivity. Selectivity is a key challenge for making ER catalysts that can convert CO_2/CO to hydrocarbons/alcohols at high turnover rates. Selectivity can be expressed in terms of faradaic efficiency (i.e., how much of the total current yields a specific product). To promote selectivity toward valuable CO_2/CO reduction products, the unwanted side reactions should be suppressed. As already mentioned, the main side reaction that should be dodged is the HER. Because HER is a very fast reaction that essentially features no overpotential, it is quite a challenging endeavor to find a catalyst that performs preferentially CO_2/CO reduction and that at a reasonable overvoltage. From pure elements,copper is the only metal that is able to produce hydrocarbons in significant amounts. Nonetheless, the reaction requires high overpotentials and is followed by high hydrogen yields. A recent theoretical study revealed the reasons for poor activity and selectivity on Cu(111).[9] Additionally, the study showed that the reduction overpotential could only be slightly decreased. The hope in the present work is that different surface geometry of the intermetallic alloys can promote selectivity and activity for the ER of CO_2/CO.

All TM assemblies in this work active for the ER of CO_2 (Ru, Co, Rh, Ir, Ni, Pd, Pt, and Cu) are also active for HER. The competition between proton discharge (reaction I) and the first electrochemical step in CO_2 reduction (reaction II) will determine the outcome of the overall reaction. In other words, the path through which the reaction proceeds depends on whether a proton prefers to bind to a free metal atom or to a CO_2 molecule adsorbed on that metal atom.

$$H^+ + e^- \rightarrow H^* \tag{I}$$

$$CO_2(g) + H^+ \rightarrow *COOH/*OCHO \tag{II}$$

The first intermediate in CO_2 reduction is either *COOH (carboxyl species) or *OCHO (formate species). To elucidate whether any of the catalysts is good for the ER of CO_2, *COOH/*OCHO and H* binding energies are plotted against each other

dx.doi.org/10.1021/cs500328c | ACS Catal. 2014, 4, 2268−2273

in Figure 3a. If CO_2 and H_2 in gas phase are used as references, then by definition, H* and *COOH/*OCHO binding free

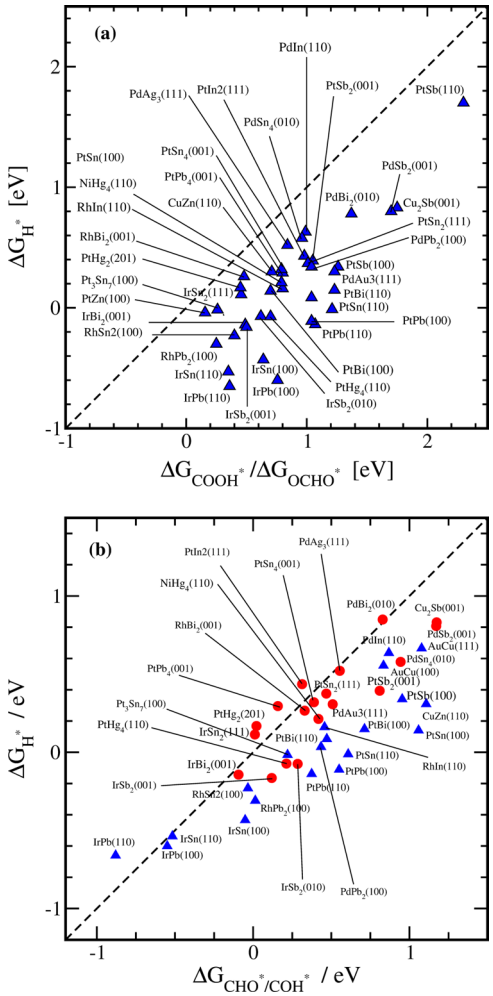

Figure 3. Free binding energies of hydrogen are plotted against (a) *COOH or *OCHO and (b) *COH or *CHO. For the points that are below, the diagonal hydrogen poisoning will prevail over CO_2/CO reduction. The intermetallic surfaces with isolated single active sites in the lower plot are denoted by red circles and those with active rows of atoms by blue triangles.

energies equal reaction free energies I and II. Therefore, hereafter, reaction energies I and II will be denoted as ΔG(H*) and ΔG(*COOH/*OCHO).

To suppress the proton discharge reaction, the points should fall in the upper part of Figure 3a, where *COOH/*OCHO binds stronger than H*, that is, ΔGCOOH*/OCHO* < ΔGH*. Apparently, ΔG (*COOH/*OCHO) is so weak that regardless of surface geometry and composition, the hydrogen poisoning always prevails. Furthermore, as both ΔG(H*) and ΔG(*COOH/*OCHO) formation steps involve transfer of one electron−proton pair, the difference between their reaction energies is not affected by the potential. It is important to stress that the inclusion of solvation effects will shift all the points to the left by ca. 0.3 eV. This means that points closest to the diagonal, for example, PtZn(100) and RhBi2(001), might after all be active for CO_2 reduction.

To turn the reaction toward CO_2 reduction products, ΔG(*COOH/*OCHO) should be increased significantly. The only way to achieve this is to raise the CO_2 pressure by several orders of magnitude. This will add up huge energy costs to already high costs associated with the reaction at large overpotentials. The entire process will therefore become economically impractical. An alternative solution is to use CO instead of CO_2. CO is an inevitable intermediate through which the ER of CO_2 must pass in order to produce hydrocarbons or alcohols. Besides, there are ways of getting CO from CO_2 both chemically and electrochemically.[49−52] Hence, if CO_2 reduction/chemical conversion to CO is coupled with CO reduction to hydrocarbons/alcohols, then the overall gain from a combined process might be as good as for the direct ER of CO_2.

The first electrochemical step in CO reduction is the formation of *COH or *CHO intermediate depending on whether hydrogen prefers to bind to the oxygen or the carbon atom. Again, the same approach is used to analyze whether CO reduction is impeded by hydrogen poisoning. As CO(g) and H_2(g) are now used as references, the reaction free energy of the first electrochemical step equals the *CHO/*COH binding free energy. Looking at Figure 3b, there are several alloy surfaces ($PtIn_2$(111), $PtHg_2$(201), $PtPb_4$(001), $PdBi_2$(111), $IrSn_2$(111) and IrPb(100)) above or close to the diagonal on which *CHO binds stronger than H*, $\Delta G_{*CHO} < \Delta G_{H*}$. The alloy surfaces just below the diagonal $PtSn_2$(111), $PtSn_4$(001), $PdAg_3$(111), $RhBi_2$(001), $IrBi_2$(001), IrSn(110) might also be selective taking into account a usual DFT error bar of 0.1 eV. Nevertheless, for the sake of brevity these alloy terminations will be left out in the following analysis. For the alloy surfaces that are far below the diagonal, the hydrogen poisoning will set in well before CO reduction commences. Selectivity appears to be highly affected by the number of atoms in the active metal assemblies. Five selective alloy surfaces have single isolated active sites, and only ItPb(100) has contiguous active sites. On surfaces with contiguous active sites, there is a possibility to make large hydrocarbon chains or to evolve hydrogen even with CO present on the surface. The coadsorption of *CO and H* on single sites is excluded because only one adsorbate can bind to a metal atom at a time.

Activity. In the introduction, we named three conditions that a good catalyst should fulfill. Stability has been included by selecting only the stable binary alloy phases. Furthermore, we have pinpointed six alloys that might be selective enough for the ER of CO. Activity is the only condition that has not been considered so far. In order to establish at which potential CO reduction takes place, it is necessary to know the potential determining step (pds) for the reaction. The pds is commonly determined by calculating the free energies of all reaction intermediates involved in the reaction. This approach entails extensive use of computer resources and time. To avoid this, we will make an assumption about the reaction's pds. The first electrochemical step (i.e., the CO protonation to either *COH or *CHO) is taken to be the pds. This assumption is reasonable given that on all calculated transition metal surfaces, this step was always found to be pds.[10] In Figure 4, ΔG(*CHO/*COH) is plotted against the corresponding energies for CO. Only for surfaces that bind CO most strongly, viz., IrPb(100), IrPb(110), and IrSn(110), ΔG(*COH) is lower compared to ΔG(*CHO). Including water stabilization will therefore not affect much the appearance of Figure 5, apart from the fact that IrPb(100), IrPb(110), and IrSn(110) points would move more to the left. The overpotential is given by the vertical distance of each point from the diagonal. The ideal catalyst with U_{OP} = 0 V by definition should lie right on the diagonal. However, as all the alloys are located far from the diagonal high overpotentials are needed to

dx.doi.org/10.1021/cs500328c | ACS Catal. 2014, 4, 2268−2273

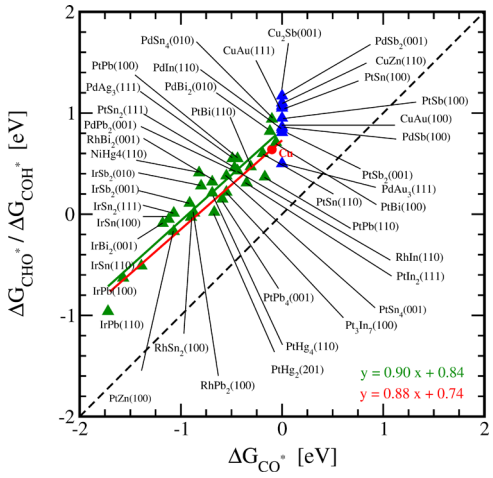

Figure 4. Free binding energies of *CHO or *COH are plotted against the corresponding energies for *CO. The green and blue triangles represent data points for intermetallic surfaces that bind and do not bind CO, respectively. The red circle stands for Cu(111). The red and blue lines are linear fits to data for the intermetallic compounds and pure transition metals, respectively. The overpotential is given by the vertical distance of each point from the diagonal.

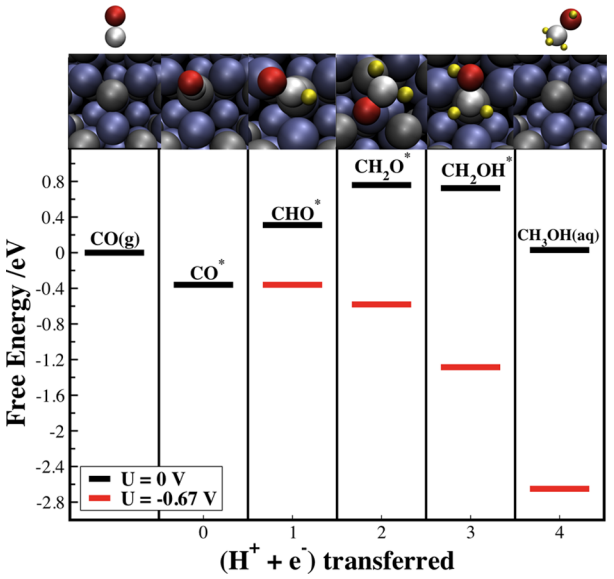

Figure 5. Free energy diagram for CO reduction on the selective and most active $PtIn_2(111)$. The black and red lines denote the free energy levels at 0 V and at the potential where all reaction steps become downhill in free energy.

reduce CO. Noteworthy is also the existence of a nice linear trend between the ΔG(*CHO/*COH) and ΔG(*CO). A trend line showing how the overpotential changes with ΔG(*CO) on metals has been included for comparison along with the Cu(111) point. According to the trends, metals and alloys exhibit very similar overpotentials. Slopes of the trend lines are slightly below 1.0, implying that the most active catalysts are predicted to be those with very weak CO binding energies (e.g, Cu(111)). Notice also that for intermetallic surfaces not binding CO (blue triangles) ΔG(*CO) is set to 0 eV. Due to a large scatter of points, certain alloys seem to be more active catalysts than metals. Starting from an initial database of 40 stable alloy surfaces (34 bulk alloys), applying the selectivity criterion reduced our pool to ca. 6 alloy surfaces that might be selective enough for CO reduction.

To determine the reaction overpotential and the final reaction product, free energy diagrams (FED) were constructed by calculating all possible reaction intermediates. The FED for the most active surface, $PtIn_2(111)$ is shown in Figure 5, whereas for other selective surfaces, FEDs are provided in Supporting Information. As initially assumed, the pds on all the alloys is the reduction of *CO to *CHO, and the final reaction product is always methanol. The most active surface is $PtIn_2(111)$ followed by $PtHg_2(201)$, $PtPb_4(001)$, $PdBi_2(111)$, and $IrSn_2(111)$, which reduce CO at potentials of −0.67, −0.69, −0.75, −0.95, and −1.08 V, respectively. For comparison purposes, the onset potential for the ER of CO on Cu was found to be −0.71 V using the same methodology as applied here.[9] It turns out that $PtIn_2(111)$ and $PtHg_2(201)$ are slightly more active than Cu(111). Furthermore, according to our analysis, these alloy surfaces are more selective in making methanol than copper is in making hydrocarbons. However, this statement should be taken with caution because we have investigated just one or at most two crystal terminations. Therefore, other reaction products cannot be a priori discarded because less dominant facets or defects can have different selectivities. In order to determine all possible products, it would be necessary to study all possible crystal terminations in a polycrystalline sample. For this reason, throughout the text we often use the term alloy surface rather than just alloy.

CONCLUSIONS

The main challenge for promoting selectivity of the ER of CO is to dodge the parasitic HER. In this work, we have proposed a new strategy that exploits the changes in geometric and electronic effects to suppress the HER. The strategy is to provide single atom centers active for the ER of CO surrounded by inactive sites for HER. It follows from our study that high faradaic efficiencies toward methanol can be achieved by removing high symmetry sites. Following this strategy, we have examined stable binary bulk alloy surfaces forming from TMs that can catalyze the reduction of CO_2 and TM or PTMs that are poor catalysts for HER. None of the catalysts was, however, selective toward the ER of CO_2. As an alternative, we proposed to reduce CO. Among the pool of binary intermetallic surfaces considered in this work (40 in total), only six, $PtIn_2(111)$, $PtHg_2(201)$, $PtPb_4(001)$, $PdBi_2(111)$, $IrSn_2(111)$, and IrPb(100), were found to be selective for CO reduction. $PtIn_2(111)$ and $PtHg_2(201)$ feature even lower reduction overpotential than Cu, which is the best known metal catalyst for the reaction. It is important to stress that this analysis is based on the (or two) most stable crystal termination(s). The product range will depend on the selectiveness of other facets. Even if these are underrepresented in polycrystalline samples, they can still account for high product yields. Another issue is that some of these alloys might be difficult to synthesize even though they are found to be thermodynamically stable.

In this work, we have introduced the concept of isolated active sites on the example of intermetallic alloys, but its implication is much broader and extends beyond one particular reaction. For instance, the same concept can be used to drive selectivities of other (electro)chemical reactions under conditions in which intermetallic alloys are stable—that is, in nonoxidizing environments and at very low or negative potentials versus RHE.

dx.doi.org/10.1021/cs500328c | ACS Catal. 2014, 4, 2268−2273

■ ASSOCIATED CONTENT

Supporting Information

Structural data for the intermetallic alloys. Free energy diagrams for the activity of selective alloys. This material is available free of charge via the Internet at http://pubs.acs.org.

■ AUTHOR INFORMATION

Corresponding Author

*E-mail: tripce@fysik.dtu.dk. Fax: (+45) 45-932-399. Tel.: (+45) 45-253-180.

Notes

The authors declare no competing financial interest.

■ ACKNOWLEDGMENTS

The Catalysis for Sustainable Energy initiative is funded by the Danish Ministry of Science, Technology, and Innovation. Support from the Danish Center for Scientific Computing, the Danish Council for Technology and Innovation's FTP program, and the Strategic Electrochemistry Research Center is gratefully acknowledged.

■ REFERENCES

(1) Lewis, N. S.; Nocera, D. G. *Proc. Natl. Acad. Sci. U.S.A.* **2006**, *103*, 15729−15735.
(2) Gattrell, M.; Gupta, N.; Co, A. *J. Electroanal. Chem.* **2006**, *594*, 1−19.
(3) Hori, Y.; Kikuchi, K.; Suzuki, S. *Chem. Lett.* **1985**, *11*, 1695−1698.
(4) Hori, Y. In *Modern Aspects of Electrochemistry*; Vayenas, C. G., White, R. E., Gamboa-Aldeco, M. E., Eds.; Springer: New York, 2008; Vol. *42*, pp 89−189.
(5) Hori, Y.; Wakebe, H.; Tsukamoto, T.; Koga, O. *Electrochim. Acta* **1994**, *39*, 1833−1839.
(6) Hori, Y.; Kikuchi, K.; Murata, A.; Suzuki, S. *Chem. Lett.* **1986**, *15*, 897−898.
(7) Hori, Y.; Murata, A.; Takahashi, R.; Suzuki, S. *J. Am. Chem. Soc.* **1987**, *109*, 5022−5023.
(8) Schouten, K. J. P.; Kwon, Y.; van der Ham, C. J. M.; Qin, Z.; Koper, M. T. M. *Chem. Sci.* **2011**, *2*, 1902.
(9) Peterson, A. A.; Abild-Pedersen, F.; Studt, F.; Rossmeisl, J.; Nørskov, J. K. *Energy Environ. Sci.* **2010**, *3*, 1311.
(10) Peterson, A. A.; Norskov, J. K. *J. Phys. Chem. Lett.* **2012**, *3*, 251−258.
(11) Li, C. W.; Kanan, M. W. *J. Am. Chem. Soc.* **2012**, *134*, 7231−7234.
(12) Markovic, N. M.; Ross, P. N. *Surf. Sci. Rep.* **2002**, *45*, 121−229.
(13) Maroun, F.; Ozanam, F.; Magnussen, O. M.; Behm, R. J. *Science* **2001**, *293*, 1811−1814.
(14) Strmcnik, D.; Escudero-Escribano, M.; Kodama, K.; Stamenkovic, V. R.; Cuesta, A.; Marković, N. M. *Nat. Chem.* **2010**, *2*, 880−885.
(15) Cuesta, A. *J. Am. Chem. Soc.* **2006**, *128*, 13332−13333.
(16) Nørskov, J. K.; Bligaard, T.; Rossmeisl, J.; Christensen, C. H. *Nat. Chem.* **2009**, *1*, 37−46.
(17) Greeley, J.; Stephens, I. E. L.; Bondarenko, A. S.; Johansson, T. P.; Hansen, H. A.; Jaramillo, T. F.; Rossmeisl, J.; Chorkendorff, I.; Nørskov, J. K. *Nat. Chem.* **2009**, *1*, 552−556.
(18) Siahrostami, S.; Verdaguer-Casadevall, A.; Karamad, M.; Deiana, D.; Malacrida, P.; Wickman, B.; Escudero-Escribano, M.; Paoli, E. A.; Frydendal, R.; Hansen, T. W.; Chorkendorff, I.; Stephens, I.; Rossmeisl, J. *Nat. Mater.* **2013**, *12*, 1137−1143.
(19) Schlapka, A.; Lischka, M.; Groß, A.; Käsberger, U.; Jakob, P. *Phys. Rev. Lett.* **2003**, *91*, 016101.
(20) Yang, R.; Leisch, J.; Strasser, P.; Toney, M. F. *Chem. Mater.* **2010**, *22*, 4712−4720.
(21) Tripković, V.; Abild-Pedersen, F.; Studt, F.; Cerri, I.; Nagami, T.; Bligaard, T.; Rossmeisl, J. *ChemCatChem* **2012**, *4*, 228−235.
(22) Bandarenka, A. S.; Varela, A. S.; Karamad, M. R.; Calle-Vallejo, F.; Bech, L.; Perez-Alonso, F. J.; Rossmeisl, J.; Stephens, I. E. L.; Chorkendorff, I. *Angew. Chem., Int. Ed.* **2012**, *51*, 11845−11848.
(23) Kitchin, J. R.; Nørskov, J. K.; Barteau, M. A.; Chen, J. G. *Phys. Rev. Lett.* **2004**, *93*, 156801.
(24) Stephens, I. E. L.; Bondarenko, A. S.; Grønbjerg, U.; Rossmeisl, J.; Chorkendorff, I. *Energy Environ. Sci.* **2012**, *5*, 6744−6762.
(25) Wang, K.; Gasteiger, H. A.; Markovic, N. M.; Ross, P. N. *Electrochim. Acta* **1996**, *41*, 2587−2593.
(26) Neurock, M.; Janik, M.; Wieckowski, A. *Faraday Discuss.* **2008**, *140*, 363−378.
(27) Neurock, M. *J. Catal.* **2003**, *216*, 73−88.
(28) Jirkovský, J. S.; Panas, I.; Ahlberg, E.; Halasa, M.; Romani, S.; Schiffrin, D. J. *J. Am. Chem. Soc.* **2011**, *133*, 19432−19441.
(29) Skúlason, E.; Tripkovic, V.; Björketun, M. E.; Gudmundsdóttir, S.; Karlberg, G.; Rossmeisl, J.; Bligaard, T.; Jónsson, H.; Nørskov, J. K. *J. Phys. Chem. C* **2010**, *114*, 18182−18197.
(30) Greeley, J.; Jaramillo, T. F.; Bonde, J.; Chorkendorff, I. B.; Nørskov, J. K. *Nat. Mater.* **2006**, *5*, 909−913.
(31) Tripkovic, V.; Vanin, M.; Karamad, M.; Björketun, M. E.; Jacobsen, K. W.; Thygesen, K. S.; Rossmeisl, J. *J. Phys. Chem. C* **2013**, *117*, 9187−9195.
(32) Calle-Vallejo, F.; Martínez, J. I.; García-Lastra, J. M.; Abad, E.; Koper, M. T. M. *Surf. Sci.* **2013**, *607*, 47−53.
(33) Mortensen, J.; Hansen, L.; Jacobsen, K. *Phys. Rev. B* **2005**, *71*, 035109.
(34) Hammer, B.; Hansen, L.; Nørskov, J. *Phys. Rev. B* **1999**, *59*, 7413−7421.
(35) Ferrin, P.; Nilekar, A. U.; Greeley, J.; Mavrikakis, M.; Rossmeisl, J. *Surf. Sci.* **2008**, *602*, 3424−3431.
(36) Nørskov, J. K.; Rossmeisl, J.; Logadottir, A.; Lindqvist, L.; Kitchin, J. R.; Bligaard, T.; Jonsson, H. *J. Phys. Chem. B* **2004**, *108*, 17886−17892.
(37) Karlberg, G. S.; Rossmeisl, J.; Nørskov, J. K. *Phys. Chem. Chem. Phys.* **2007**, *9*, 5158−5161.
(38) Rossmeisl, J.; Nørskov, J. K.; Taylor, C. D.; Janik, M. J.; Neurock, M. *J. Phys. Chem. B* **2006**, *110*, 21833−21839.
(39) Abild-Pedersen, F.; Andersson, M. P. *Surf. Sci.* **2007**, *601*, 1747−1753.
(40) Mason, S. E.; Grinberg, I.; Rappe, A. M. *Phys. Rev. B* **2004**, *69*, 161401.
(41) Kresse, G.; Gil, A.; Sautet, P. *Phys. Rev. B* **2003**, *68*, 73401.
(42) Stamenkovic, V.; Mun, B. S.; Mayrhofer, K. J. J.; Ross, P. N.; Markovic, N. M.; Rossmeisl, J.; Greeley, J.; Nørskov, J. K. *Angew. Chem., Int. Ed.* **2006**, *45*, 2897−2901.
(43) Oloman, C.; Li, H. *ChemSusChem* **2008**, *1*, 385−391.
(44) Marković, N. M.; Grgur, B. N.; Ross, P. N. *J. Phys. Chem. B* **1997**, *101*, 5405−5413.
(45) Pourbaix, M. *Atlas of Electrochemical Equilibria in Aqueous Solutions*, 2nd, ed.; National Association of Corrosion Engineers: Houston, TX, 1974.
(46) Christoffersen, E.; Stoltze, P.; Nørskov, J. K. *Surf. Sci.* **2002**, *505*, 200−214.
(47) Menning, C. A.; Hwu, H. H.; Chen, J. G. *J. Phys. Chem. B* **2006**, *110*, 15471−15477.
(48) Andersson, K. J.; Calle-Vallejo, F.; Rossmeisl, J.; Chorkendorff, I. *J. Am. Chem. Soc.* **2009**, *131*, 2404−2407.
(49) Hansen, H. A.; Varley, J. B.; Peterson, A. A.; Nørskov, J. K. *J. Phys. Chem. Lett.* **2013**, *4*, 388−392.
(50) Rakowski DuBois, M.; DuBois, D. L. *Acc. Chem. Res.* **2009**, *42*, 1974−1982.
(51) Hori, Y.; Murata, A.; Kikuchi, K.; Suzuki, S. *J. Chem. Soc., Chem. Commun.* **1987**, 728.
(52) Higman, C.; van der Burgt, M. *Gasification*, 2nd ed.; Gulf Professional Publishing: Oxford, 2008.